March, 1990] © *1990 The Chemical Society of Japan* *Bull. Chem. Soc. Jpn.*, ***63***, *877—885 (1990)* 877

Thermal Decompositions of CH_3I and CD_3I. Experimental and Theoretical Approaches to the Specific Rates at the High Pressure Limit

Sukeya KODAMA* and Yasuhiro OOI
Department of Applied Chemistry, College of Engineering, University of Osaka Prefecture, Sakai, Osaka 591

(Received April 8, 1989)

The rate constants on the thermal decompositions of CH_3I and CD_3I at the high pressure limit, k_d^∞, were evaluated from the decomposition rates, measured as functions of the reaction time and the pressure of methyl iodide. The values of $k_d^\infty(CH_3I)$ at 606.8, 620.2, 633.5, and 649.5 K were 2.92, 8.22, 22.0, and $68.2\times10^{-6}\ s^{-1}$, respectively. The values of $k_d^\infty(CD_3I)/k_d^\infty(CH_3I)$ were 0.290 at 620.2 K, 0.285 at 633.5 K, and 0.279 at 649.5 K. Meanwhile, the calculations for k_d^∞ were carried out using a rate theory derived from the assumption that the zero point energy and the vibrational energy are concerned in the entropy term of k_d^∞. From good correspondence between the experimental and calculated values, the values of D_0 (chemical bond dissociation energy)=243.7, ΔE_0 (energy change at 0 K)=230.6, and ΔH_{298}° (enthalpy change at 298 K)=236.3 kJ mol^{-1} were obtained for the CH_3–I bond dissociation. On the decomposition of equimolar mixture of CH_3I and CD_3I at 633.5 K and 10.67 kPa of the total pressure, it was found that the initial rate ratio of $R^\circ(CH_4+CH_3D)/R^\circ(CD_4+CD_3H)$ is 1.94 and the excitations to the active molecules of CH_3I and CD_3I in the mixture are less effective than those in the separated systems of CH_3I and CD_3I, respectively.

Methyl iodide is one of such molecules that the experimental and theoretical approaches for the unimolecular decomposition rate are easy by the following reasons: the bond dissociation energy of the C–I bond is considerably low as compared with those of the C–C and C–H bonds of hydrocarbons; so, it is easy to control the reaction and to obtain the rate constant at the high pressure limit, because the decomposition proceeds at relatively low temperatures; the reaction mechanism is simple, because the main hydrocarbon product is methane only; the presumption of activated complex model and the theoretical calculation are easy.

On the thermal decomposition of CH_3I, Butler and Polanyi[1] have studied the pyrolysis of CH_3I in N_2 of about 820 Pa and obtained 2.33 to $7.80\times10^{-2}\ s^{-1}$ as the rate constant at 767 K. Horrex and Lapage[2] have reported that the rate constant depends strongly on the total pressure and is $2.8\times10^{-2}\ s^{-1}$ at 800 K and 80.5 kPa. They have also obtained the rate expression of $k_d(s^{-1})=2.6\times10^{13}\exp\{-54.7(\text{kcal mol}^{-1})/RT\}$. Saito et al.[3] have investigated the thermal decomposition of CH_3I diluted in Ar by means of the behind shock waves in the temperature range from 1050 to 1500 K and the total density range of 3.5×10^{-6} to 3.9×10^{-5} mol cm^{-3}. They have found that the initiation reaction is the C–I bond fission, the rate constant decreases by decreasing of the total density, and the rate constant at the low pressure limit is given by $k_{2nd}(cm^3mol^{-1}\ s^{-1})=10^{15.40}\exp\{-42.56(\text{kcal mol}^{-1})/RT\}$. Saito et al.[4] have also reported that the pre-exponential term of k_{2nd} is $10^{15.0}$ for Kr and $10^{15.88}\ cm^3mol^{-1}\ s^{-1}$ for He from the pyrolysis of CH_3I diluted in Kr and He.

Since both pre-exponential and exponential terms of the rate constant vary with the pressure of the system,[5] the experimental determination of the rate constant at the high pressure limit is desirable to obtain the thermodynamic values such as the bond dissociation energy and the enthalpy change of reaction. However, the experimental rate constants cited above are not the values at the high pressure limit. On the other hand, a rate theory was derived by considering the contribution to the entropy term of rate constant of the zero point energies and the vibrational energies.[5] In order to examine the propriety of the rate theory, it is advisable to study the kinetic isotope effect together with the adaptability to the experimental rate constants at the high pressure limit. From these points of view, the pyrolyses of CH_3I and CD_3I were carried out in this work.

Experimental

The reaction cell used for the pyrolysis was a quartz cylinder of 5.0 cm innner diameter and 11.5 cm length, with a volume of 227.5 cm^3. The reaction cell was inserted into a copper vessel with a thickness of 9 mm to make temperature uniform in the reaction cell. The copper vessel was set in a cylindrical electric furnace which can be heated from three sides of the lower, middle, and upper parts to reduce the temperature gradient in the furnace. The reaction temperature was observed using a chromel–alumel thermocouple which was corrected with the melting points of Bi, Hg_2Cl_2, Pb, $PbBr_2$, CdI_2, Zn, AgCl, LiI, $PbCl_2$, LiBr, and $CdCl_2$. The temperature in the cell was kept within ±0.5 K during the reaction period.

CH_3I obtained from Wako Pure Chemicals was above 98.0% in purity. CD_3I was obtained from Merk Japan, and its minimum extent of deuterium was 99%. Both samples were purified each time before use by means of condensation and evacuation at 77 K.

The main products in the pyrolysis of CH_3I were CH_4 and I_2. Trace formations of C_2H_6, C_2H_4, and C_2H_2 were also found. The iodine-contained hydrocarbons could not be detected in the gas chromatographic analysis using a Porapak Q column (3 m) at 428 K. The reaction products in the pyrolysis of CD_3I were also the same as those for CH_3I.

The thermal decomposition was carried out by introducing CH_3I or CD_3I into the reaction cell maintained at a fixed temperature. After reaction, the reaction mixture was removed to a trap at 77 K. Methane, passing through the trap, was collected in a Toepler gauge, and its amount was determined. The degree of conversion of methyl iodide which was estimated from the ratio of the twofold amount of formed methane to the introduced amount of methyl iodide was less than 2.8% for CH_3I and 4.7% for CD_3I. The pyrolysis of equimolar mixture of CH_3I and CD_3I was also carried out by the same procedure as mentioned above. The separation of methanes was performed using a mass spectrometer (Hitachi, RMU-6E) at the ionizing voltage of 16 eV.

The vibrational wavenumbers of CD_3I in the vapor phase were observed by an infrared spectrometer.

Results

The amonnt of CH_4 forming in the pyrolysis of CH_3I, V_{CH_4}, was measured as functions of the reaction temperature, the pressure of CH_3I, and the reaction time (t). The results are shown in Table 1. The results

Table 1. Formation Amount of CH_4 from CH_3I, Measured as Functions of the Reaction Temperature, the Pressure of CH_3I, and the Reaction Time

606.8 K		620.2 K		633.5 K		649.5 K	
Reaction time/min	V_{CH_4}/μmol	Reaction time/min	V_{CH_4}/μmol	Reaction time/min	V_{CH_4}/μmol	Reaction time/min	V_{CH_4}/μmol
5.33 kPa		2.60 kPa		5.33 kPa		5.33 kPa	
20	0.357	12	0.154	10	0.815	6	0.978
28	0.515	42	0.566	13	0.929	7	1.08
40	0.724	62	0.787	20	1.37	9	1.37
60	0.932	6.80 kPa		30	1.82	15	2.18
10.67 kPa		12	0.703	10.67 kPa		25	3.05
20	0.784	24	1.13	10	1.89	10.67 kPa	
40	1.32	36	1.76	20	2.89	5	2.24
60	1.88	54	1.94	30	4.05	15	4.88
16.00 kPa		14.39 kPa		16.00 kPa		16.00 kPa	
20	1.23	10	2.13	10	3.28	5	3.43
40	2.27	20	2.46	20	4.81	15	7.53
60	3.00	30	4.24	30	6.50	21.33 kPa	
21.33 kPa		45	4.29	21.33 kPa		5	4.71
20	1.82	24.26 kPa		10	4.50	15	10.4
40	3.36	8	3.03	20	6.50	30	17.8
60	4.13	16	4.50	30	7.89		
		24	6.58				
		38	7.23				

Table 2. Formation Amount of CD_4 from CD_3I, Measured as Functions of the Reaction Temperature, the Pressure of CD_3I, and the Reaction Time

620.2 K		633.5 K		649.5 K		665.5 K		681.5 K	
Reaction time/min	V_{CD_4}/μmol	Reaction time/min	V_{CD_4}/μmol	Reaction time/min	V_{CD_4}/μmol	Reaction time/min	V_{CD_4}/μmol	Reaction time/min	V_{CD_4}/μmol
5.33 kPa		5.33 kPa		5.33 kPa		5.33 kPa		5.33 kPa	
20	0.381	12	0.459	10	0.742	5	0.893	3	1.17
40	0.759	20	0.730	15	1.04	12	1.89	9	3.09
60	1.23	40	1.20	25	1.75	15	2.33	15	4.62
10.67 kPa		48	1.51	30	2.09	10.67 kPa		10.67 kPa	
20	0.861	60	1.87	10.67 kPa		5	1.96	3	2.45
40	1.34	10.67 kPa		10	1.47	11	3.73	9	5.95
60	2.01	15	0.980	16	2.11	15	4.64	15	9.70
16.00 kPa		30	1.65	30	3.35	16.00 kPa		16.00 kPa	
20	1.21	45	2.32	16.00 kPa		5	2.81	3	3.48
40	1.85	16.00 kPa		10	2.63	10	4.34	5	4.76
60	2.57	15	1.32	16	3.51	15	6.54	9	8.40
21.33 kPa		30	2.62	30	5.20	21.33 kPa		15	15.1
20	1.53	45	3.47	21.33 kPa		5	3.76	21.33 kPa	
40	2.53	21.33 kPa		10	3.45	9	5.32	3	5.16
60	3.71	10	1.28	16	4.47	15	9.05	7	8.55
		15	1.62	30	7.11			9	10.8
		27	2.97					15	19.0
		45	4.82						

for CD_3I measured with the same procedure are shown in Table 2. As an example, the relations of V_{CH_4} versus t in the pyrolysis of CH_3I at 633.5 K are shown in Fig. 1, and it is found that the slope of V_{CH_4} to t decreases with an increase of the reaction time. This trend was found in all cases.

The initial formation rates of methanes were determined by using various empirical equations. As an instance, the equation

$$V_{CH_4} = at/(1 + bt^{0.8})$$

was used for the pyrolysis of CH_3I at 633.5 K, where a and b mean the initial formation rate and a suppression factor for the methane formation, respectively. Above equation can be rewritten as

$$t/V_{CH_4} = 1/a + (b/a)t^{0.8}.$$

The plots of t/V_{CH_4} versus $t^{0.8}$ are shown in Fig. 2 and the initial formation rates ($R^{\circ}_{CH_4}$) were obtained from the intercepts.

The initial formation rates obtained by these procedures are shown in Fig. 3 for CH_3I and in Fig. 4 for CD_3I as functions of the reaction temperature and the concentration of methyl iodide. It is found in both figures that the initial formation rate increases with higher order than the first order for the concentration of methyl iodide.

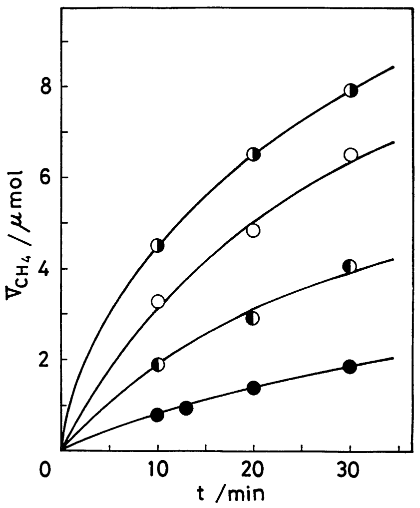

Fig. 1. Formation amount of CH_4, measured as a function of the reaction time in the pyrolysis of CH_3I at 633.5 K. ●, 5.33 kPa; ◐, 10.67 kPa; ○, 16.00 kPa; ◑, 21.33 kPa.

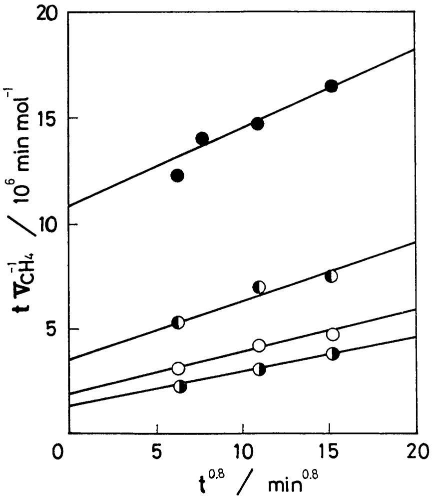

Fig. 2. Plots of t/V_{CH_4} versus $t^{0.8}$ in the pyrolysis of CH_3I at 633.5 K. ●, 5.33 kPa; ◐, 10.67 kPa; ○, 16.00 kPa; ◑, 21.33 kPa.

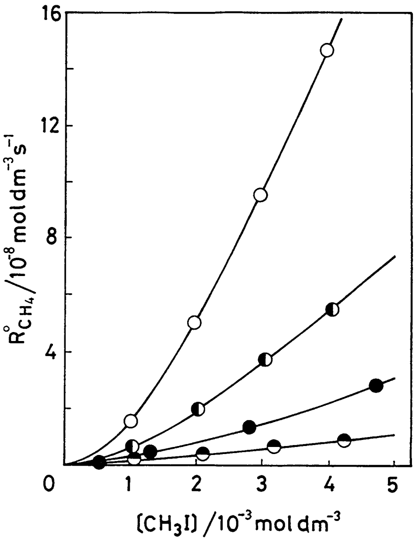

Fig. 3. Plots of $R^{\circ}_{CH_4}$ versus [CH_3I]. ◒, 606.8 K; ●, 620.2 K; ◐, 633.5 K; ○, 649.5 K.

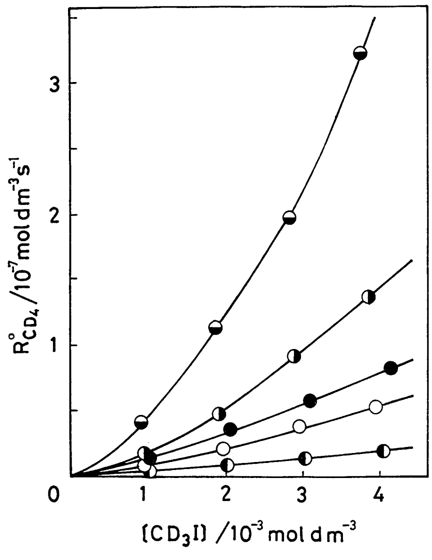

Fig. 4. Plots of $R^{\circ}_{CD_4}$ against [CD_3I]. ●, 620.2 K ($R^{\circ}_{CD_4}$×10); ◐, 633.5 K; ○, 649.5 K; ◑, 665.5 K; ◒, 681.5 K.

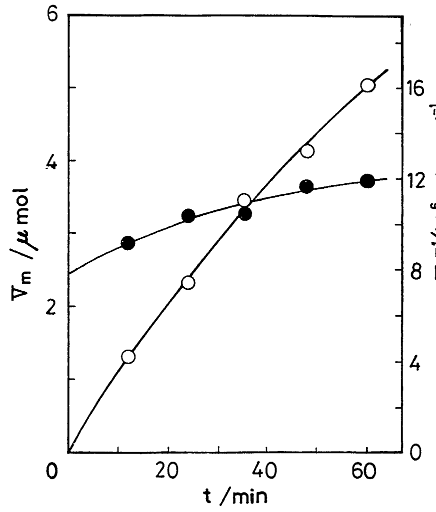

Fig. 5. Plots of V_m and t/V_m versus t in the pyrolysis of equimolar mixture of CH_3I and CD_3I at 633.5 K and the total pressure of 10.67 kPa. ○, V_m; ●, t/V_m.

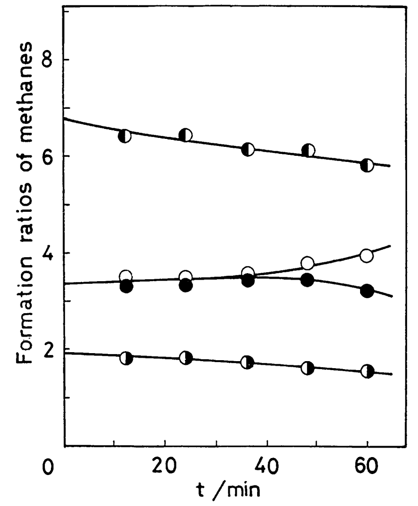

Fig. 6. Plots of the formation ratios of methanes against the reaction time in the pyrolysis of equimolar mixture of CH_3I and CD_3I at 633.5 K. ◐, R_{CH_4}/R_{CD_4}; ○, R_{CHD_3}/R_{CD_4}; ●, R_{CH_4}/R_{CH_3D}; ◑, $R(CH_4+CH_3D)/R(CD_4+CHD_3)$.

The pyrolysis of equimolar mixture of CH_3I and CD_3I was carried out at 633.5 K and the total pressure of 10.67 kPa. Plots of the total formation amount of methanes (V_m) and t/V_m versus t are shown in Fig. 5. The initial rate for the total formation of methanes, R_m°, was found to be 9.35×10^{-12} mol ml^{-1} s^{-1} from the intercept of the t/V_m vs. t curve. Plots of R_{CH_4}/R_{CD_4}, R_{CHD_3}/R_{CD_4}, R_{CH_4}/R_{CH_3D}, and $R(CH_4+CH_3D)/R(CD_4+CHD_3)$ against t are shown in Fig. 6. Both initial rate ratios of R_{CH_4}/R_{CH_3D} and R_{CHD_3}/R_{CD_4} were found to be about 3.4 from the intercepts.

Discussion

Reaction Mechanism and Kinetics. From the results obtained above, the following mechanism was postulated for the main reactions in the pyrolysis of CH_3I, where CH_3I^* and $CH_3I^{\ddagger}$ mean the active molecule and the activated complex, respectively:

$$CH_3I + CH_3I \longrightarrow CH_3I + CH_3I^* \tag{1}$$

$$CH_3I^* + CH_3I \longrightarrow CH_3I + CH_3I \tag{2}$$

$$CH_3I^* \longrightarrow CH_3I^{\ddagger} \tag{3}$$

$$CH_3I^{\ddagger} \longrightarrow CH_3I^* \tag{4}$$

$$CH_3I^{\ddagger} \longrightarrow CH_3 + I \tag{5}$$

$$CH_3 + CH_3I \longrightarrow CH_4 + CH_2I. \tag{6}$$

Iodine atoms and CH_2I radicals formed by Reactions 5 and 6 seem to disappear by the self-dimerization and cross-combination reactions

$$I + I \xrightarrow{M} I_2$$

$$I + CH_2I \xrightarrow{(M)} CH_2I_2$$

$$CH_2I + CH_2I \xrightarrow{(M)} C_2H_4I_2,$$

where M is a deactivator molecule. The formation rate of CH_4 decreases with increasing of the reaction time as is seen in Fig. 1. This suppression may be due to the reactions of CH_3 radicals with I and I_2 which were accumulated during the pyrolysis.[6]

$$CH_3 + I \xrightarrow{(M)} CH_3I$$

$$CH_3 + I_2 \longrightarrow CH_3I + I$$

The trace formations of C_2H_6, C_2H_4, and C_2H_2 seem to be caused by the reactions such as $CH_3+CH_2I \rightarrow C_2H_5+I$, $C_2H_5+CH_3I \rightarrow C_2H_6+CH_2I$, $2CH_3 \rightarrow C_2H_6$, $CH_3+CH_2I \rightarrow C_2H_4+HI$, $C_2H_4I_2 \rightarrow C_2H_4+I_2$, and $C_2H_4I_2 \rightarrow C_2H_2+2HI$. The reaction mechanism for the pyrolysis of CD_3I appears to be the same as that for CH_3I.

From the mechanism of Reactions 1—6, the initial rate for the formation of methane is given by

$$R_{CH_4}^\circ = \frac{k_1k_3k_5[CH_3I]^2}{k_3k_5 + k_2(k_4 + k_5)[CH_3I]}. \tag{7}$$

Equation 7 can be rewritten as

$$\frac{[CH_3I]}{R_{CH_4}^\circ} = \frac{1}{k_d} = \frac{1}{k_d^\infty} + \frac{1}{k_1[CH_3I]}. \tag{8}$$

Here, k_d^∞ means the rate constant at the high pressure limit, and it is given by

$$k_d^\infty = \frac{k_1 k_3 k_5}{k_2(k_4 + k_5)}. \tag{9}$$

Plots of $[CH_3I]/R^\circ_{CH_4}$ versus $1/[CH_3I]$ are shown in Fig. 7. Figure 8 shows the relations of $[CD_3I]/R^\circ_{CD_4}$ against $1/[CD_3I]$. The values of k_d^∞ obtained from the intercepts in Figs. 7 and 8 and the ratio of $k_d^\infty(CD_3I)/k_d^\infty(CH_3I)$ are shown in Table 3.

Kinetic Isotope Effect. On the basis of Reactions 1—6, the following reaction mechanism was postulated for the formation of methanes in the pyrolysis of mixture of CH_3I and CD_3I:

$$CH_3I + CH_3I \text{ or } CD_3I \underset{k_{2a}}{\overset{k_{1a}}{\rightleftharpoons}} CH_3I^* + CH_3I \text{ or } CD_3I$$

$$CD_3I + CH_3I \text{ or } CD_3I \underset{k_{2b}}{\overset{k_{1b}}{\rightleftharpoons}} CD_3I^* + CH_3I \text{ or } CD_3I$$

$$CH_3I^* \underset{k_{4a}}{\overset{k_{3a}}{\rightleftharpoons}} CH_3I^{\ddagger} \xrightarrow{k_{5a}} CH_3 + I$$

$$CD_3I^* \underset{k_{4b}}{\overset{k_{3b}}{\rightleftharpoons}} CD_3I^{\ddagger} \xrightarrow{k_{5b}} CD_3 + I$$

$$CH_3 + CH_3I \longrightarrow CH_4 + CH_2I \tag{6a}$$

$$CH_3 + CD_3I \longrightarrow CH_3D + CD_2I \tag{6b}$$

$$CD_3 + CH_3I \longrightarrow CD_3H + CH_2I \tag{6c}$$

$$CD_3 + CD_3I \longrightarrow CD_4 + CD_2I. \tag{6a}$$

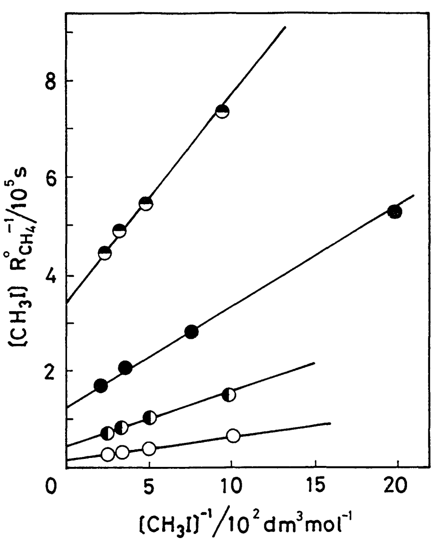

Fig. 7. Plots of $[CH_3I]/R^\circ_{CH_4}$ versus $1/[CH_3I]$. ◓, 606.8 K; ●, 620.2 K; ◐, 633.5 K; ○, 649.5 K.

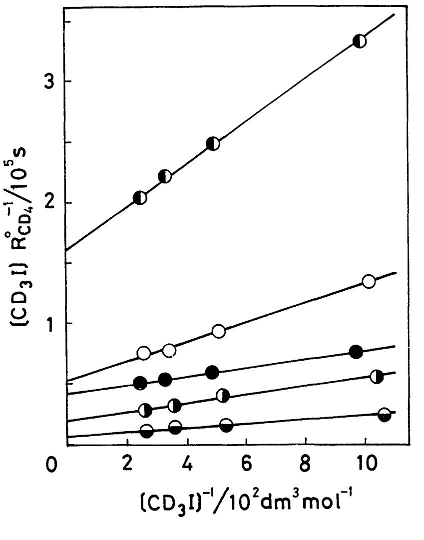

Fig. 8. Plots of $[CD_3I]/R^\circ_{CD_4}$ versus $1/[CD_3I]$. ●, 620.2 K; $(([CD_3I]/R^\circ_{CD_4})/10)$; ◐, 633.5 K; ○, 649.5 K; ◑, 665.5 K; ◒, 681.5 K.

From the mechanism of Reactions 1a—6d, the decomposition rates of CH_3I and CD_3I, $R^\circ_d(CH_3I)_m$ and $R^\circ_d(CD_3I)_m$, can be estimated from the relations of

$$R^\circ_d(CH_3I)_m = R^\circ_m\,\alpha/(1+\alpha) \tag{10}$$

and

$$R^\circ_d(CD_3I)_m = R^\circ_m/(1+\alpha). \tag{11}$$

Here, $R^\circ_m = R^\circ_{CH_4} + R^\circ_{CH_3D} + R^\circ_{CD_3H} + R^\circ_{CD_4}$ and α is given by

$$\alpha = (R^\circ_{CH_4} + R^\circ_{CH_3D})/(R^\circ_{CD_3H} + R^\circ_{CD_4}). \tag{12}$$

When the experimental values of $R^\circ_m = 9.35$ pmol ml^{-1} s^{-1} and $\alpha = 1.94$ at 633.5 K and 10.67 kPa of the total pressure were applied to Eqs. 10 and 11, $R^\circ_d(CH_3I)_m = 6.17$ and $R^\circ_d(CD_3I)_m = 3.18$ pmol ml^{-1} s^{-1} were obtained.

On the other hand, the initial decomposition rate of CH_3I at 633.5 K and 10.67 kPa of CH_3I only, $R^\circ_d(CH_3I)$, was 20.76 pmol ml^{-1} s^{-1}. Since the mole fraction of CH_3I in the mixture is one half, the ratio of the initial decomposition rate of CH_3I in the mixture to that of CH_3I only, $\eta(CH_3I)$, was estimated to be 0.594 from the relation

$$\eta(CH_3I) = 2R^\circ_d(CH_3I)_m/R^\circ_d(CH_3I).$$

Similarly, the ratio of the initial decomposition rate of CD_3I in the mixture to that of CD_3I only, $\eta(CD_3I)$, was evaluated to be 0.772 using the relation

Table 3. Experimental Values of $k_d^\infty(CH_3I)$, $k_d^\infty(CD_3I)$, and $k_d^\infty(CD_3I)/k_d^\infty(CH_3I)$

T K	$k_d^\infty(CH_3I)$ 10^{-6} s^{-1}	$k_d^\infty(CD_3I)$ 10^{-6} s^{-1}	$k_d^\infty(CD_3I)$ $k_d^\infty(CH_3I)$
606.8	2.92		
620.2	8.22	2.38	0.290
633.5	22.0	6.27	0.285
649.5	68.2	19.0	0.279
665.5		54.5	
681.5		149	

$$\eta(\mathrm{CD_3I}) = 2R^\circ_\mathrm{d}(\mathrm{CD_3I})_\mathrm{m}/R^\circ_\mathrm{d}(\mathrm{CD_3I}).$$

and $R^\circ_\mathrm{d}(\mathrm{CD_3I})$=8.24 pmol ml^{-1} s^{-1} at 633.5 K and 10.67 kPa of $\mathrm{CD_3I}$ only.

These results suggest that both excitations to the active molecules of $\mathrm{CH_3I}$ and $\mathrm{CD_3I}$ by cross-collisions in the mixture are less effective than those in the separated systems of $\mathrm{CH_3I}$ and $\mathrm{CD_3I}$.

On the other hand, the exchange reactions between $\mathrm{CH_3}$ and $\mathrm{CD_3}$ radicals by the iodine atom abstraction from methyl iodide are conceivable in the pyrolysis of the mixture of $\mathrm{CH_3I}$ and $\mathrm{CD_3I}$.

$$\mathrm{CH_3 + CD_3I} \underset{k_{13\mathrm{b}}}{\overset{k_{13\mathrm{a}}}{\rightleftharpoons}} \mathrm{CD_3 + CH_3I} \tag{13}$$

Since the relations of $R^\circ_\mathrm{d}(\mathrm{CH_3I})_\mathrm{m} > R^\circ_\mathrm{d}(\mathrm{CD_3I})_\mathrm{m}$ and hence $[\mathrm{CH_3}] > [\mathrm{CD_3}]$ exist in this system, the reaction to shift to the right side seems to proceed. The shift leads to the increase of $\eta(\mathrm{CD_3I})$ and the decrease of $\eta(\mathrm{CH_3I})$. Accordingly, if we assume $k_{13\mathrm{a}}/(k_{6\mathrm{a}}+k_{6\mathrm{b}}) = k_{13\mathrm{b}}/(k_{6\mathrm{c}}+k_{6\mathrm{d}})$, the value of $k_{13\mathrm{a}}/(k_{6\mathrm{a}}+k_{6\mathrm{b}})$ can be estimated from the equation

$$\frac{k_{13\mathrm{a}}}{k_{6\mathrm{a}}+k_{6\mathrm{b}}} = \frac{\beta-\alpha}{(\alpha-1)(\beta+1)}, \tag{14}$$

where β means the ratio of the real decomposition rate of $\mathrm{CH_3I}$ to that of $\mathrm{CD_3I}$ in the mixture. When the values of $\beta = R^\circ_\mathrm{d}(\mathrm{CH_3I})/R^\circ_\mathrm{d}(\mathrm{CD_3I}) = 2.52$ ($\eta(\mathrm{CH_3I}) = \eta(\mathrm{CD_3I}) = 0.645$) and $\alpha = 1.94$ were applied to Eq. 14, the value of $k_{13\mathrm{a}}/(k_{6\mathrm{a}}+k_{6\mathrm{b}})$ was 0.175.

The result suggests that the rate of iodine abstraction is fairly slow as compared with the rate of hydrogen abstraction, though the exchange between $\mathrm{CH_3}$ and $\mathrm{CD_3}$ radicals by the iodine abstraction is conceivable.

On the formations of $\mathrm{CH_4}$, $\mathrm{CH_3D}$, $\mathrm{CHD_3}$, and $\mathrm{CD_4}$, the rate expressions

$$R^\circ_{\mathrm{CH_4}}/R^\circ_{\mathrm{CH_3D}} = k_{6\mathrm{a}}/k_{6\mathrm{b}} \tag{15}$$

and

$$R^\circ_{\mathrm{CHD_3}}/R^\circ_{\mathrm{CD_4}} = k_{6\mathrm{c}}/k_{6\mathrm{d}} \tag{16}$$

can be derived when $[\mathrm{CH_3I}]$ is equal to $[\mathrm{CD_3I}]$. Both experimental values of $k_{6\mathrm{a}}/k_{6\mathrm{b}}$ and $k_{6\mathrm{c}}/k_{6\mathrm{d}}$ were found to be 3.4 from Fig. 6.

On the other hand, the wavenumber of doubly degenerate stretching vibration of the C–H bond of $\mathrm{CH_3I}$ is 3060.3 cm^{-1},[7] and the wavenumber for $\mathrm{CD_3I}$ is 2160 cm^{-1}. Therefore, the difference between the zero point energies of the vibrations becomes 5385 J mol^{-1}. If the zero point energy is assumed to contribute to the enthalpy term of the rate constant of the hydrogen abstraction reaction,[8] the rate constant ratio of $k_{6\mathrm{a}}/k_{6\mathrm{b}}$ or $k_{6\mathrm{c}}/k_{6\mathrm{d}}$ seems to depend on the factor of exp $(5385/RT)$, and the factor at 633.5 K was 2.8. Therefore, the kinetic isotope effect on the rate constant ratios appears to be caused mainly by the zero point energy difference, judging from the experimental value of $k_{6\mathrm{a}}/k_{6\mathrm{b}}$ or $k_{6\mathrm{c}}/k_{6\mathrm{d}}$ and the factor. Similar results were also found on the hydrogen abstraction reactions by $\mathrm{CH_3}$ or $\mathrm{CD_3}$ from $\mathrm{H_2}$ or $\mathrm{D_2}$,[9] by $\mathrm{CD_3}$ from $\mathrm{C_2H_6}$ or $\mathrm{C_2D_6}$,[10] and others.[11]

Thermodynamic Considerations. The enthalpy change of the thermal decomposition

$$\mathrm{CH_3I(g)} \longrightarrow \mathrm{CH_3(g) + I(g)}$$

at 298 K, $\Delta H^\circ_{298}(\mathrm{CH_3I})$, is given by

$$\Delta H^\circ_{298}(\mathrm{CH_3I}) = \Delta H^\circ_{\mathrm{f},298}(\mathrm{CH_3(g)}) + \Delta H^\circ_{\mathrm{f},298}(\mathrm{I(g)}) - \Delta H^\circ_{\mathrm{f},298}(\mathrm{CH_3I(g)}) \tag{17}$$

using the standard heat of formation ($\Delta H^\circ_{\mathrm{f},298}$). The energy change at 0 K, $\Delta E_0(\mathrm{CH_3I})$, can be calculated from the equation

$$\Delta E_0(\mathrm{CH_3I}) = \Delta H^\circ_{298}(\mathrm{CH_3I}) - RT\left[\frac{5}{2} + \left(\sum_{i=1}^{6}\frac{x_i}{\mathrm{e}^{x_i}-1}\right)_{\mathrm{CH_3}} - \left(\sum_{i=1}^{9}\frac{x_i}{\mathrm{e}^{x_i}-1}\right)_{\mathrm{CH_3I}}\right] \tag{18}$$

derived using the principle of the equipartition of energy for the translational and rotational energies, $RT\sum x_i/(\exp x_i - 1)$ for the vibrational energy, and $\Delta H = \Delta E + \Delta nRT$. Here, $x_i = hc\bar{\nu}_i/kT$ and $\bar{\nu}_i$ means the wavenumber of i-th vibration.[5]

The dissociation energy at 0 K, $D_0(\mathrm{CH_3{-}I})$, can be calculated from

$$D_0(\mathrm{CH_3{-}I}) = \Delta E_0(\mathrm{CH_3I}) + \Delta E^\ddagger_\mathrm{z}(\mathrm{CH_3I}), \tag{19}$$

where

$$\Delta E^\ddagger_\mathrm{z}(\mathrm{CH_3I}) = E_\mathrm{z}(\mathrm{CH_3I}) - E^\ddagger_\mathrm{z}(\mathrm{CH_3}) = \left(\sum_{i=1}^{8} hc\bar{\nu}_i/2\right)_{\mathrm{CH_3I}} - \left(\sum_{i=1}^{6} hc\bar{\nu}^\ddagger_i/2\right)_{\mathrm{CH_3}}. \tag{20}$$

Here, $E_\mathrm{z}(\mathrm{CH_3I})$ means the total sum of zero point energies for all vibrations except for the stretching vibration of the $\mathrm{CH_3{-}I}$ bond. $E^\ddagger_\mathrm{z}(\mathrm{CH_3})$ denotes the over-all zero point energy for the vibrations of $\mathrm{CH_3}$.

When the wavenumbers listed in Table 4 for the vibrations of $\mathrm{CH_3I}$ and $\mathrm{CH_3}$, and the thermochemical values of $\Delta H^\circ_{\mathrm{f},298}(\mathrm{CH_3I(g)}) = 13.8$, $\Delta H^\circ_{\mathrm{f},298}(\mathrm{CH_3(g)}) = 143.2$,[5] and $\Delta H^\circ_{\mathrm{f},298}(\mathrm{I(g)}) = 106.9$[12] kJ mol^{-1} are adopted, the values of $\Delta E_0(\mathrm{CH_3I}) = 230.6$ and $D_0(\mathrm{CH_3{-}I}) = 243.7$ kJ mol^{-1} were obtained from Eqs. 18 and 19. The value of $\Delta H^\circ_{\mathrm{f},298}(\mathrm{CH_3I(g)})$ adopted above seems to be reasonable, judging from the reported values of 9.6,[13] 13.8,[14] 14.2,[15] and 15.9[16] kJ mol^{-1}.

The value of $D_0(\mathrm{CD_3{-}I})$ can be estimated from the

Table 4. Physical Constants for the Molecules and the Activated Complexes on the Thermal Decompositions of CH_3I and CD_3I

	Molecule		Complex	
	CH_3I	CD_3I	$(CH_3\cdots I)^{\neq}$	$(CD_3\cdots I)^{\neq}$
Wavenumber/cm^{-1}	533.2(1)[a] 882.7(2) 1250.8(1) 1438.2(2) 2953.2(1) 3060.3(2)	491(1)[a] 514(2) 940(1) 964(2) 2085(1) 2160(2)	617(1) 1396(2) 3044(1) 3162(2)	463(1) 1026(2) 2513(1) 2381(2)
Moment of inertia/10^{-47} kg m^2	5.52(1) 111.5(2)	11.02(1) 138.6(2)	5.85(1) 2.92(2)	11.68(1) 5.84(2)

a) Stretching vibration of the C–I bond.

relation

$$D_0(CD_3\text{–}I) = D_0(CH_3\text{–}I) + hc[\bar{\nu}_{st}(CH_3I) - \bar{\nu}_{st}(CD_3I)]/2, \qquad (21)$$

where $\bar{\nu}_{st}$ means the wavenumber of the C–I stretching vibration. $\Delta E_0(CD_3I)$ can be calculated by the equation

$$\Delta E_0(CD_3I) = D_0(CD_3\text{–}I) - [E_z(CD_3I) - E_z^{\neq}(CD_3)]. \qquad (22)$$

The value of $E_z(CD_3I) - E_z^{\neq}(CD_3)$ can be estimated by the same equation as Eq. 20 for CH_3I. By using the wavenumbers listed in Table 4 and $D_0(CH_3\text{–}I)$ obtained above, the values of $D_0(CD_3\text{–}I)=244.0$ and $\Delta E_0(CD_3I)=240.9$ kJ mol^{-1} were obtained from Eqs. 21 and 22.

Calculations and Comparisons of k_d^∞. The calculations of k_d^∞ for the thermal decompositions of CH_3I and CD_3I were carried out using the equation

$$k_d^\infty = \frac{kT}{h}\frac{q_r^{\neq} q_{ir}^{\neq} e^{-D_0/RT}}{q_r q_v}\int_0^\infty e^{\Delta S_v^{\neq}/R} e^{-E_c/RT} d\left(\frac{E_e}{RT}\right) \qquad (23)$$

derived previously.[5)] The activated complex for a single-bond fission should be very loose, because it must have the same structure as that for the radical-radical recombination which is a reverse reaction. Thus, the Gorin model[17)] which free methyl radical and iodine atom are in an associated state by the intermolecular force was adopted. The physical constants for the molecules and the activated complexes based on the Gorin model are shown in Table 4 for the wavenumbers of vibrations of CH_3I,[7)] CD_3I,[18)] CH_3,[19)] and CD_3,[19)] and the moments of inertia of the rotations of CH_3I,[20)] CD_3I,[20)] CH_3,[21)] and CD_3.[21)]

The rotational partition function of the activated complex, $q_r^{\neq}$, is given by

$$q_r^{\neq} = \frac{8\pi^2\Gamma(2/3)\mu kT}{\sigma^{\neq} h^2}\left(\frac{2A}{kT}\right)^{1/3}, \qquad (24)$$

when the Gorin model can be adopted for the complex.[22)] Here, μ, $\sigma^{\neq}$, and Γ denote the reduced mass, the symmetry number, and the gamma function, respectively. Since both free CH_3 (CD_3) radical (planar, D_{3h}) and I atom are nonpolar, the attractive potential constant in the Lennard-Jones 12–6 intermolecular potential, A, can be calculated from the Slater and Kirkwood equation for the dispersion term.[5,23)] The value of A calculated using the values of $\alpha(CH_3)=\alpha(CD_3)=2.24\times10^{-30}$ m^3,[24)] $\alpha(I)=5.04\times10^{-30}$ m^3,[24)] and $N_e(CH_3)=N_e(CD_3)=N_e(I)=7$ for the polarizability (α) and the number of outer-shell electrons (N_e) was 2.01×10^{-77} J m^6.

The vibrational energy accumulated in all vibrations of methyl iodide except for the stretching vibration of the C–I bond, E_e, can be calculated from the equation

$$E_e = RT\sum_{i=1}^{8} x_i/(e^{x_i} - 1). \qquad (25)$$

Meanwhile, the vibrational energy which is carried in the activated complex, $E_v^{\neq}$, is given by the relation[5)]

$$E_v^{\neq} = \Delta E_z^{\neq} - 3RT/2 + E_e. \qquad (26)$$

The vibrational temperature in the complex, $T_v^{\neq}$, can be estimated by the procedure described previously.[5)] It is found in Fig. 9 that $T_v^{\neq}$ is considerably higher than the reaction temperature (T). As is found from the relation of Eq. 26, the main contributions to $T_v^{\neq}$ in the lower and higher temperature ranges are due to $\Delta E_z^{\neq}$ and E_e, respectively. The increase of $T_v^{\neq}(CH_3I) - T_v^{\neq}(CD_3I)$ by decreasing of T is based on the relation of $\Delta E_z^{\neq}(CH_3I) > \Delta E_z^{\neq}(CD_3I)$. Meanwhile, the proximity of $T_v^{\neq}(CD_3I)$ to $T_v^{\neq}(CH_3I)$ by increasing of T is caused by $E_e(CD_3I) > E_e(CH_3I)$.

The value of $\Delta S_v^{\neq}$ can be calculated using Eqs. 27—29

$$\Delta S_v^{\neq} = S_v^{\neq} - S_v^{*} \qquad (27)$$

$$S_v^{*} = R\sum_{i=1}^{8}[x_i/(e^{x_i} - 1) - \ln(1 - e^{-x_i})] \qquad (28)$$

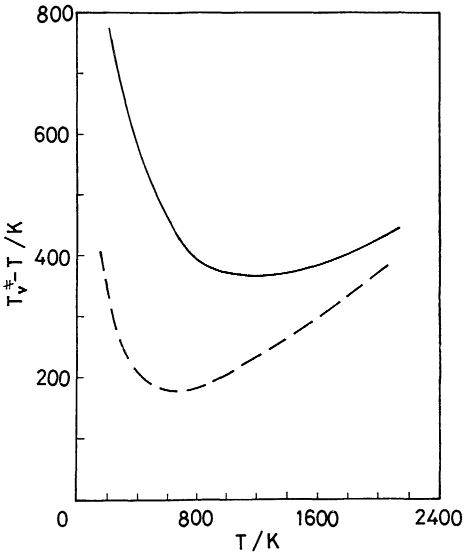

Fig. 9. Relations of the vibrational temperature in the activated complex ($T_v^{\ddagger}$) and the reaction temperature (T). —, CH_3I; – –, CD_3I.

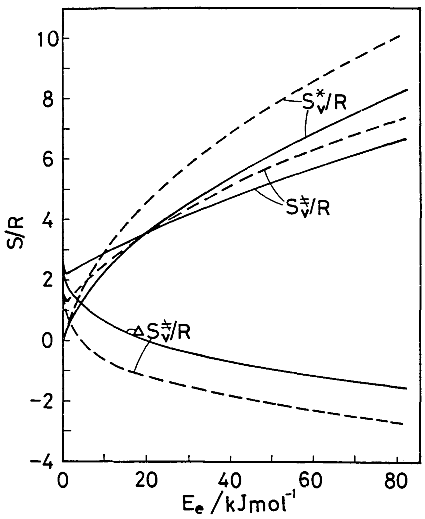

Fig. 10. Plots of S_v^*/R, $S_v^{\ddagger}/R$, and $\Delta S_v^{\ddagger}/R$ as a function of E_e. —, CH_3I; – –, CD_3I.

Table 5. Calculated Values of $k_d^\infty(CH_3I)$, $k_d^\infty(CD_3I)$, and $k_d^\infty(CD_3I)/k_d^\infty(CH_3I)$

T / K	$k_d^\infty(CH_3I)$ / s^{-1}	$k_d^\infty(CD_3I)$ / s^{-1}	$k_d^\infty(CD_3I)$ / $k_d^\infty(CH_3I)$
400	3.88×10^{-17}	1.59×10^{-17}	0.404
600	1.70×10^{-6}	5.02×10^{-7}	0.293
800	2.87×10^{-1}	6.40×10^{-2}	0.222
1000	3.28×10^{2}	5.76×10^{1}	0.175
1200	3.08×10^{4}	4.40×10^{3}	0.143
1600	6.48×10^{6}	6.93×10^{5}	0.107

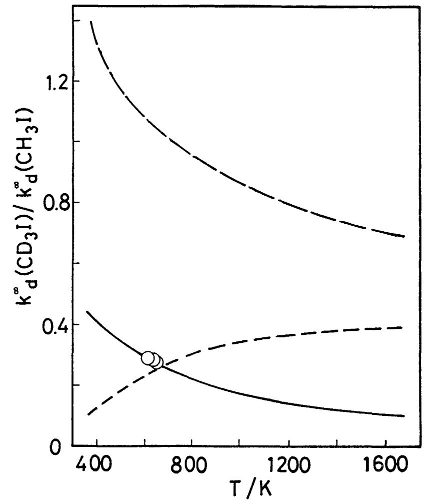

Fig. 11. Temperature dependence of $k_d^\infty(CD_3I)/k_d^\infty(CH_3I)$. Calculated value: —, calculated using Eq. 23; – –, the RRKM theory; – – –, the theory of absolute reaction rates. Experimental value: ○, the present work.

$$S_v^{\ddagger} = R\sum_{i=1}^{6}[x_i^{\ddagger}/(e^{x_i^{\ddagger}} - 1) - \ln (1 - e^{-x_i^{\ddagger}})], \qquad (29)$$

where $x_i^{\ddagger}=hc\bar{\nu}_i^{\ddagger}/kT_v^{\ddagger}$. Here, $\bar{\nu}_i^{\ddagger}$ denotes the wavenumber of i-th vibration of the complex.

The values of S_v^*, $S_v^{\ddagger}$, and $\Delta S_v^{\ddagger}$ calculated using the procedure described previously5) are shown in Fig. 10 as a function of E_e. Both values of E_e and S_v^*/R at 0 K are zero. While, the values of $S_v^{\ddagger}/R$ and $\Delta S_v^{\ddagger}/R$ at $E_e=0$ have positive value, because $\Delta E_z^{\ddagger}$ and $E_v^{\ddagger}$ at 0 K are positive from the relation of Eq. 26. However, it is seen in Fig. 10 that $\Delta S_v^{\ddagger}/R$ decreases with an increase of E_e, because S_v^*/R increases more rapidly than $S_v^{\ddagger}/R$.

The values of $k_d^\infty(CH_3I)$, $k_d^\infty(CD_3I)$, and $k_d^\infty(CD_3I)/k_d^\infty(CH_3I)$ calculated from Eq. 23 using the values in Table 4, $D_0(CH_3\text{-}I)=243.7$, and $D_0(CD_3\text{-}I)=244.0$ kJ mol^{-1} are shown in Table 5. The calculations of $k_d^\infty(CH_3I)$, $k_d^\infty(CD_3I)$, and $k_d^\infty(CD_3I)/k_d^\infty(CH_3I)$ on the basis of the theory of absolute reaction rates25) and the RRKM theory26) were also carried out using the same activated complex model, the physical constants listed in Table 4, the values of D_0 exhibited above, $\Delta E_0(CH_3I)=230.6$, and $\Delta E_0(CD_3I)=240.9$ kJ mol^{-1}, in the same way as the calculations for the thermal decompositions of methanes and ethanes.5)

Figure 11 shows the calculated values of $k_d^\infty(CD_3I)/k_d^\infty(CH_3I)$ together with the experimental values. It is found in Fig. 11 that the values calculated using Eq. 23 are in well accord with the experimental values, but the values calculated with the RRKM theory are too high compared with the experimental values.

The Arrhenius plots for the calculated values of $k_d^\infty(CH_3I)$ are shown in Fig. 12 together with those for the experimental values, where the experimental values1–4) except for the values in the present work are

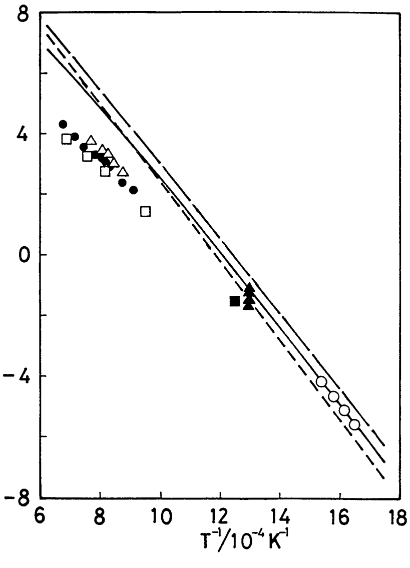

Fig. 12. Plots of log $k_\mathrm{d}^\infty(\mathrm{CH_3I})$ versus $1/T$. Calculated value: —, calculated using Eq. 23; – – –, the RRKM theory; — —, the theory of absolute reaction rates. Experimental value: ○, the present work; ▲, Ref. 1 (ca. 820 Pa); ■, Ref. 2 (80.5 kPa); □, Ref. 3 (5.8 μmol cm^{-3}); ●, Ref. 3 (13.2 μmol cm^{-3}); △, Ref. 3 (27.3 μmol cm^{-3}). All experimental values except for those in the present work (○) are not the rate constant at the high pressure limit.

not those at the high pressure limit. In Fig. 12, it is found that the values calculated using Eq. 23 consist fully with the experimental values in the present work, and the values calculated with the theory of absolute reaction rates are fairly high compared with the experimental values. The increase of k_d^∞ depends mainly on the decrease of the enthalpy term of k_d^∞ by the relation of $\Delta E_0=D_0-\Delta E_z^\ddagger$ in Eq. 19. This fact suggests that $\Delta E_z^\ddagger$ participates in the entropy term of k_d^∞, but is not related to the enthalpy term.⁵⁾

The temperature dependence of $k_\mathrm{d}^\infty(\mathrm{CH_3I})$ calculated by the RRKM theory is fairly high compared with that calculated from Eq. 23 in common with those on the thermal decompositions of $\mathrm{CH_4}$ and $\mathrm{C_2H_6}$.⁵⁾ Therefore, the conformity with the experimental values grows worse in the lower and higher temperature ranges as is seen in Fig. 12.

References

1) E. T. Butler and M. Polanyi, *Trans. Faraday Soc.*, **39**, 19 (1943).

2) C. Horrex and R. Lapage, *Disc. Faraday Soc.*, **10**, 233 (1951).

3) K. Saito, H. Tahara, O. Kondo, T. Yokubo, T. Higashihara, and I. Murakami, *Bull. Chem. Soc. Jpn.*, **53**, 1335 (1980).

4) K. Saito, H. Tahara, and I. Murakami, *Bull. Chem. Soc. Jpn.*, **57**, 3023 (1984).

5) S. Kodama, *Bull. Chem. Soc. Jpn.*, **63**, 867 (1990).

6) F. K. Truby and J. K. Rice, *Int. J. Chem. Kinet.*, **5**, 721 (1973); T. F. Hunter and K. S. Kristjansson, *J. Chem. Soc., Faraday Trans. 2*, **78**, 2067 (1982); S. P. Pardini and D. S. Martin, *Int. J. Chem. Kinet.*, **15**, 1031 (1983).

7) G. Herzberg, "Molecular Spectra and Molecular Structure.III. Electronic Spectra and Electronic Structure of Polyatomic Molecules, "Van Nostrand Reihold, New York (1966), p. 621.

8) K. J. Laidler, "Chemical Kinetics," 2nd ed, McGraw-Hill, New York (1965), p. 90; P. Gray, A. A. Herod, and A. Jones, *Chem. Rev.*, **71**, 247 (1971).

9) E. Whittle and E. W. R. Steacie, *J. Chem. Phys.*, **21**, 993 (1953); J. S. Shapiro and R. E. Weston, *J. Phys. Chem.*, **76**, 1669 (1972); N. L. Arthur, K. F. Donchi, and J. A. McDonell, *J. Chem. Soc., Faraday Trans. 1*, **71**, 2431 (1975).

10) W. M. Jackson, J. R. McNesby, and B. de B. Darwent, *J. Chem. Phys.*, **37**, 1610 (1962).

11) N. L. Arthur and J. A. McDonell, *J. Chem. Phys.*, **57**, 3228 (1972); G. D. Beverly and R. M. Martin, *J. Phys. Chem.*, **80**, 2063 (1976); N. Fujisaki, A. Ruf, and T. J. Gäumann, *J. Chem. Soc., Faraday Trans. 2*, **83**, 2053 (1987).

12) W. H. Evans, T. R. Munson, and D. D. Wagman, *J. Research Natl. Bur. Standards*, **55**, 147 (1955); "JANAF Interim Thermochemical Tables," Thermal Laboratory, Dow Chemical Co., Midland, Mich. (1960).

13) M. C. Flowers and S. W. Benson, *J. Chem. Phys.*, **38**, 882 (1963).

14) D. M. Golden, R. Walsh, and S. W. Benson, *J. Am. Chem. Soc.*, **87**, 4053 (1965).

15) C. A. Goy and H. O. Pritchard, *J. Phys. Chem.*, **69**, 3040 (1965).

16) A. S. Carson, W. Carter, and J. B. Pedley, *Proc. R. Soc. London, Ser. A*, **260**, 550 (1961).

17) E. Gorin, *Acta Physicochim. URSS*, **9**, 681 (1938); E. Gorin, W. Kauzmann, J. Walter, and H. Eyring, *J. Chem. Phys.*, **7**, 633 (1939).

18) Observed by an infrared spectrometer.

19) A. Snelson, *J. Phys. Chem.*, **74**, 537 (1970).

20) Calculated using r(C–H)=1.096 Å, r(C–I)=2.139 Å, and ∠HCI=107.0°.

21) Calculated using r(C–H)=1.079 Å and ∠HCH=120° in p. 609 of Ref. 7.

22) E. V. Waage and B. S. Rabinovitch, *Chem. Rev.*, **70**, 377 (1970).

23) J. C. Slater and J. G. Kirkwood, *Phys. Rev.*, **37**, 682 (1931); J. G. Kirkwood, *Physik. Z.*, **33**, 57 (1932).

24) Estimated from $\alpha(\mathrm{H_2})=0.802$, $\alpha(\mathrm{CH_4})=2.63$, $\alpha(\mathrm{C_2H_6})=4.49$, and $\alpha(\mathrm{HI})=5.44\times10^{-30}\,\mathrm{m}^3$.

25) S. Glasstone, K. J. Laidler, and H. Eyring, "The Theory of Rate Processes," McGraw-Hill, New York (1941); K. J. Laidler and M. C. King, *J. Phys. Chem.*, **87**, 2657 (1983).

26) R. A. Marcus, *J. Chem. Phys.*, **20**, 355, 359, 364 (1952); B. S. Rabinovitch and D. W. Setser, *Adv. Photochem.*, **3**, 1 (1964).